Radical strain-release photocatalysis for the synthesis of azetidines

Ricardo I. Rodríguez[1], Vasco Corti[1], Lorenzo Rizzo[1], Stefano Visentini[1], Marco Bortolus[1], Agnese Amati[2], Mirco Natali[2], Giorgio Pelosi[3], Paolo Costa[1], and Luca Dell'Amico[1*]

[1]Department of Chemical Sciences, University of Padova, Via Francesco Marzolo 1, 35131 Padova, Italy.

[2]Department of Chemical and Pharmaceutical Sciences, University of Ferrara, Via Luigi Borsari 46, 44121 Ferrara, Italy.

[3]Department of Chemistry, Life Sciences and Environmental Sustainability, Parco Area delle Scienze 17, 43124 Parma, Italy.

Abstract

The increasing popularity of four-member rings in drug discovery programs has vastly widen the research in synthetic chemistry, guiding the community to progress and reinvent old strategies for their crafting. Recently, the strain-release concept has been effectively used to build complex architectures. However, in contrast to the tens of described strategies accessing small carbocyclic derivatives, *azetidine* synthesis remains severely underdeveloped. Here, we report a mild visible-light-driven method to access densely functionalised azetidines by subjecting azabicyclo[1.1.0]butanes (ABBs) to radical strain-release (RSR) photocatalysis. We investigated the mechanism of this process using a combination of spectroscopic and optical techniques, and density functional theory (DFT) calculations. The chemistry is orchestrated by the activity of a novel organic photosensitiser, that governs the key energy-transfer process with diverse types of sulfonylimine precursors. The formed radical intermediates are intercepted by the ABB through an RSR process, leading access to azetidines in high chemical yields in a single operation. The power and generality of this photocatalytic method is demonstrated for various azetidine targets, including derivatives of Celecoxib and Naproxen.

Introduction

Nitrogen-containing heterocycles are one of the most abundant classes of molecules present in drugs and agrochemicals[1-3]. While planar systems, such as pyridine and derivatives still play a major role, the scientific community is currently exploring alternative molecular architectures that display elevated three-dimensionality and high degree of sp^3-hybridized carbon atoms (Fsp^3)[4,5]. This trend is sustained by their increased metabolic stability and structural modularity with respect to the planar systems[6,7]. Because of its documented ability to mimic pyridine, piperidine and pyrrolidine for bioisosteric replacement purposes, the azetidine core highlights as a privileged scaffold (Figure 1a)[8,9]. This is of major importance in drug design, as more than 60% of the currently marketed pharmaceuticals contain at least one N-heterocycle[10]. Nevertheless, despite its promising pharmacokinetic properties over five- and six-membered nitrogen rings, azetidines only count nine approved drugs (Figure 1b)[11-14]. The discrepancy between importance and prevalence of azetidine-bearing molecules is likely attributed to their challenging synthesis.

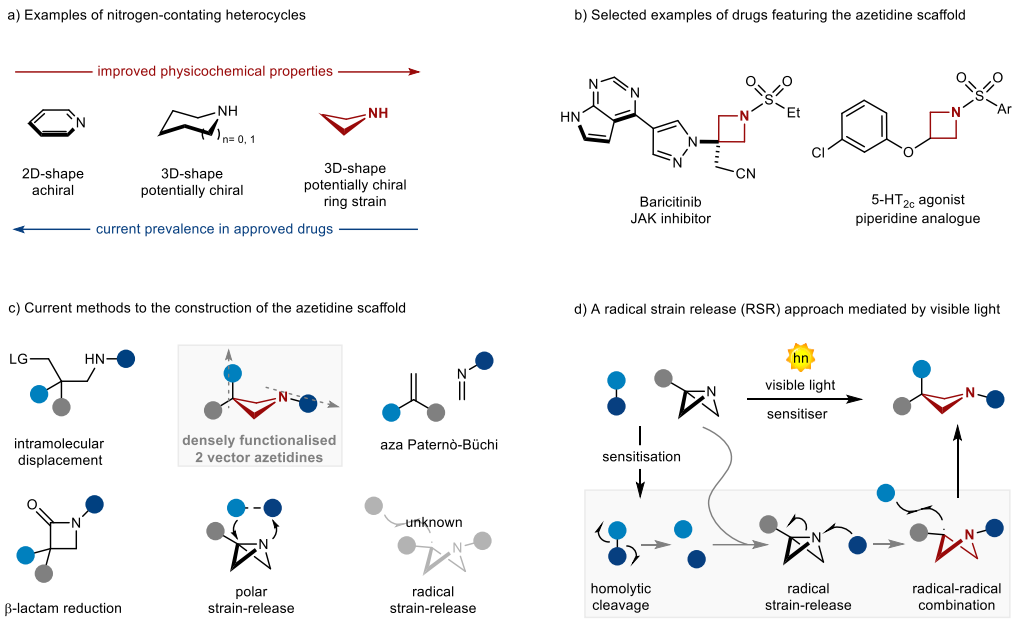

Fig. 1. a) Relevance of the azetidine scaffold and current prevalence in approved drugs. b) Selected examples of drugs featuring the azetidine core. c) Available synthetic strategies for the construction of the azetidine core. d) Development of a radical strain-release synthetic method, and general mechanism.

Classical approaches involve intramolecular nucleophilic substitution (S_n2) reactions[15-17], or lactam reduction[18-19] (Figure 1c). However, severe limitations still prevent the general application of such methods, including the low functional group tolerance and the need of tailored precursors. More recently, the aza-Paternò-Büchi reaction has been popularized and used to access complex azetidines[20-24]. This is arguably a milder synthetic approach compared to the previously mentioned. It generally requires visible light and the presence of commercially available photocatalysts (PCs). However, the reaction not always displays high levels of regio- and diastereoselectivity, and its stereochemical outcome is hard to predict. An alternative paradigm deals with the use of strained 1-azabicyclo[1.1.0]butanes (ABBs)[25-31]. This strained molecule can undergo a double functionalization process in presence of an electrophile (blue circle) and a nucleophile (azure circle)[27-29], with the predictable formation of two new bonds in a single synthetic operation. Nonetheless, the generality of this process is hampered by the need of using specific electrophilic partner and/or strong acidic conditions[30,31].

With only a handful of synthetic methods available, the identification of a general approach to access the azetidine core will be highly impactful on the organic and medicinal chemistry communities. In particular, a radical strategy based on the strain-release of ABB is still missing to date. Such an approach, while unlocking uncharted radical reactivity, will lead access to new azetidine variants expanding the synthetic repertoire for azetidine constructions. Fortunately, over the last decades photocatalysis has been established as one of the pillars in synthetic catalysis, introducing new reactivities and nonobvious retrosynthetic disconnections[32-37]. In this panorama, RSR photocatalysis has recently emerged as a formidable tool for the construction of small rings[38].

Here, we report the development of a radical light-driven method that transforms readily available ABBs into densely functionalized azetidines (Figure 1d). The strategy relies on the activity of a sensitizer that promotes the homolytic cleavage of a large variety of sulfonylimine precursors. The two generated radical intermediates (azure and blue circles) react with the ABB leading to its chemoselective double functionalization, without the need of any ABB activation step. This mechanism was thoroughly investigated with a series of spectroscopic and optical techniques and supported by DFT calculations. With the gathered experimental and spectroscopic evidence on the transiently generated C-centred radical, we report an advantageously designed three-component version of the reaction, leading access to a variety of complex azetidine systems while maintaining high yields and complete chemoselectivity. Selected product manipulations highlight the relevance of our strategy for accessing key azetidine cores present in biologically relevant molecules[39]. By using this RSR process it is possible to construct simultaneously a nitrogen-sulfur bond with diverse types of sulfonyl groups while installing a nitrogen or a sulfur atom at position C3 (azure circle in Figure 1d), thus accessing not only a hindered fully substituted carbon centre but also securing the presence of two well-defined exit vectors[40].

Results and discussion.

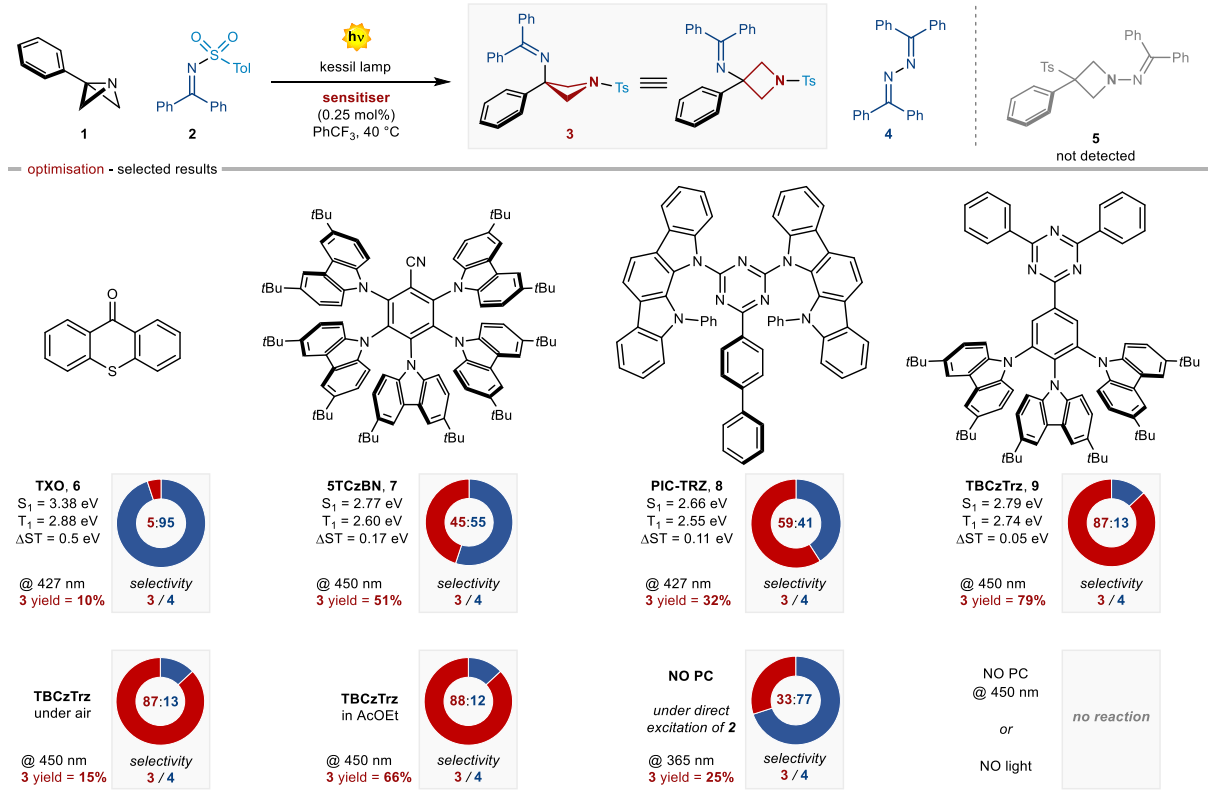

Fig. 2. Selected results from the reaction optimisation process. The reported yields refer to the average of isolated products obtained from three independent reactions. Reactions performed at 0.05 mmol scale (see Supporting Information for details). TXO = Thioxanthen-9-one, 5TCzBN = 2,3,4,5,6-penta-(9*H*-carbazol-9-yl)benzonitrile, PIC-TRZ = 2-biphenyl-4,6-bis(12-phenylindolo[2,3-a] carbazole-11-yl)-1,3,5-triazine, TBCzTrz = 9,9',9''-(5-(4,6-Diphenyl-1,3,5-triazin-2-yl)benzene-1,2,3-triyl)tris(3,6-di-tert-butyl-9*H*-carbazole)

We began our study investigating the reaction between the Ph-ABB **1** and the sulfonylimine **2**. After a series of unsuccessful results (see Supporting Information, section 2), we found out that thioxanthone (TXO) **6** afforded the azetidine product **3** in 10% yield, along with major amount of imine dimer **4**. This result indicates that the concentration of the iminyl radical in the reaction mixture is critical. We thus reasoned that slowing down the iminyl radical formation would channel the reactivity towards the formation of the target azetidine **3**[41,42]. To this end, we investigated different classes of sensitisers, characterized by a high T_1 $E_{0,0}$ (> 2.55 eV), and a very small ΔST (Figure 2 and Supporting Information, section 2.3)[43]. This last parameter accounts for a rapid S_1-T_1 and T_1-S_1 interconversion through intersystem crossing (ISC) and reversed intersystem crossing (RISC), respectively. We hypothesised that a small ΔST together with an efficient RISC would downregulate the concentration of the PC's T_1 state in solution, controlling the imine sensitization and preventing the possible formation of **4**. Indeed, we observed a consistent trend between the ΔST value and the selectivity of the process towards the azetidine **3** vs imine dimer **4** (Figure 2 and Supporting Information, section 2.3). It is worth mentioning that, also other parameters can influence the selectivity of the process, including the sensitizer loading, which was kept as low as 0.25 mol%, the λ max and the PC's absorption tail, as well as the PC's solubility (see Supporting Information, Section 2). Taken all these aspects in consideration, we found the best performance for the PC **9**, characterized by the lowest ΔST of 0.05 eV, and a T_1 $E_{0,0}$ = 2.74 eV. Intriguingly, across all the performed reactions we never observed the formation of the reversed product isomer **5**, where the sulfonyl group is attached at C3 position (vide infra).

We next investigated the mechanism of this RSR process (Figure 3a). We initially assessed the feasibility of an EnT step between the excited sensitizer **9** and the sulfonylimine **2**. Luminescence quenching studies confirmed that the excited state of the sensitizer is effectively quenched by the sulfonylimine **2**, whereas negligible quenching is observed with the ABB **1** (Figure 3b). Then, we focused on the homolytic cleavage of the N-S bond with the formation of the radicals **10** and **11**. Such radical intermediates are proposed to react with the ABB **1** in a chemoselective manner to deliver the final N-Ts azetidine **3**. To gain insights in these steps, we performed laser flash photolysis (LFP) analyses. Interestingly, under 355 nm direct excitation of **2**, we observed the development of a transient absorption centred at 410 nm (Figure 3c and S35 left in the Supporting Information), mainly associated with the tosyl radical **10**[44,45]. In the absence of other reagents, this species decays to the baseline within a few μs, due to radical recombination. In the presence of **1**, a similar transient species is immediately detected upon excitation (Figure 3c, red traces). However, a new transient species subsequently arises, which is characterized by an absorption maximum at 435 nm and a pronounced tail at longer wavelengths. These transient changes can be reasonably assigned to the formation of the radical intermediate **12**. Consistent with this attribution, the associated positive absorption, measured at 450 nm (Figure S35 bottom in the Supporting Information), increases with the concentration of the ABB **1**, as expected based upon the bimolecular nature of the radical reaction between **10** and **1**. The subsequent decay, occurring within ca 10 μs, can be finally assigned to the reaction of **12** with radical **11** and concurrent formation of the final product **3**.

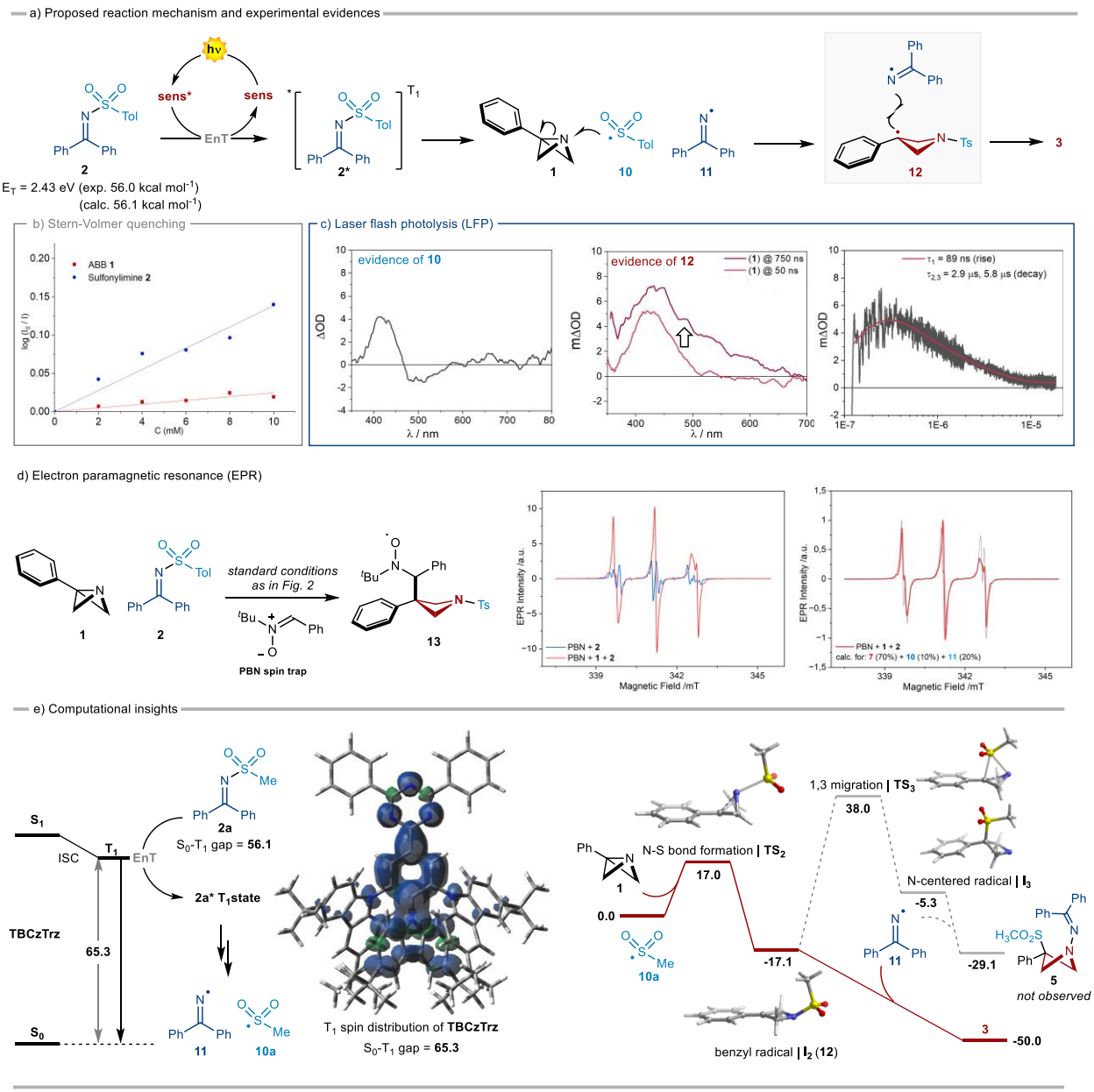

Fig. 3. a) Proposed reaction manifold with experimental support from b) luminescence quenching studies; c) laser flash photolysis (LFP); and d) electron paramagnetic resonance (EPR) studies. All values are reported in kcal·mol^{-1}.PBN = *N-tert*-butyl-α-phenylnitrone.

To further corroborate the mechanistic proposal while gathering more information about the key intermediate **12**, we performed electron paramagnetic resonance (EPR) experiments in presence of the spin trapping reagent *N-tert*-butyl-α-phenylnitrone (PBN) and the PC **9**. We firstly explored the homolytic cleavage of **2** in the absence of the ABB **1**. Under these conditions, we detected the information of mixed radical species clearly identifying two main species (Figure 3d, blue trace). The parameters of the EPR spectrum are consistent with the trapping of an N-centred and an S-centred radicals in equal proportions, thus suggesting that these species are the sulfonyl and iminyl radicals **10** and **11**. When performing the spin trapping experiment under the reaction conditions (in the presence of **1**), a more intense and completely different spectrum was obtained

(Figure 3d, red trace). This spectrum suggests that multiple radical species are trapped, but the main trapped radical – about the 70% – is compatible with the carbon-centred radical **12**. It is worth noting that, the reaction with PBN in the absence of **1** and **2** shows no radical formation confirming that these reagents are the only source of the radical species under the reaction mixture. (For more details see Supporting Information, section 5.3).

Finally, we performed DFT calculations at the (U)M062x/def2TZVP level of theory including a solvent model (IEFPCM, solvent= toluene) to evaluate the energetic profile of the reaction and rationalise the observed chemoselectivity. To optimize computational resources, a sulfonylimine featuring a mesyl group instead of the bulkier tosyl group was selected (**2a**, Figure 3e). In agreement with the findings from Stern-Volmer quenching studies, the energy transfer (EnT) process between the photocatalyst and the sulfonylimine is determined to be exergonic, with a calculated Gibbs free energy change (ΔG) of -9.1 kcal mol^{-1} (Figure 3e, left). An examination of the spin density distribution map of the relaxed triplet state of **TBCzTrz 9** suggests that the EnT mechanism likely initiates through a collision complex involving the triazine moiety of the photocatalyst and the sulfonylimine **2**. Next, the generation of the sulfonyl **10a** and iminyl radical **11**, resulting from the homolytic cleavage of the sulfonylimine's N-S bond is determined to be exergonic (ΔG = -10.3 kcal mol^{-1}). This step is accompanied by a relatively modest activation barrier, with $\Delta G^{\ddagger}$ = 8.1 kcal mol^{-1} (Figure 3e, right). Hence, we computed the insertion mechanism of the sulfonyl radical **10a** into the C-N bond of the ABB **1**, followed by radical-radical recombination with the iminyl radical **11**, ultimately yielding the final product isomer **5**. Intriguingly, although a transition state (TS_2, $\Delta G^{\ddagger}$ = 17.0 kcal mol^{-1}) is identified between intermediate I_2 (the benzyl radical similar to **12**) and the initial reactants **1** and **10a**, a direct transition state between intermediate I_3 (N-centred radical) and the reactants **1** and **10a** proved elusive. Instead, a substantial energy barrier (TS_3, $\Delta G^{\ddagger}$ = 55.1 kcal mol^{-1}) is calculated between I_2 and TS_3, explaining the experimental absence of the structural product isomer **5**, coupled with its lower thermodynamic stability compared to product **3**.

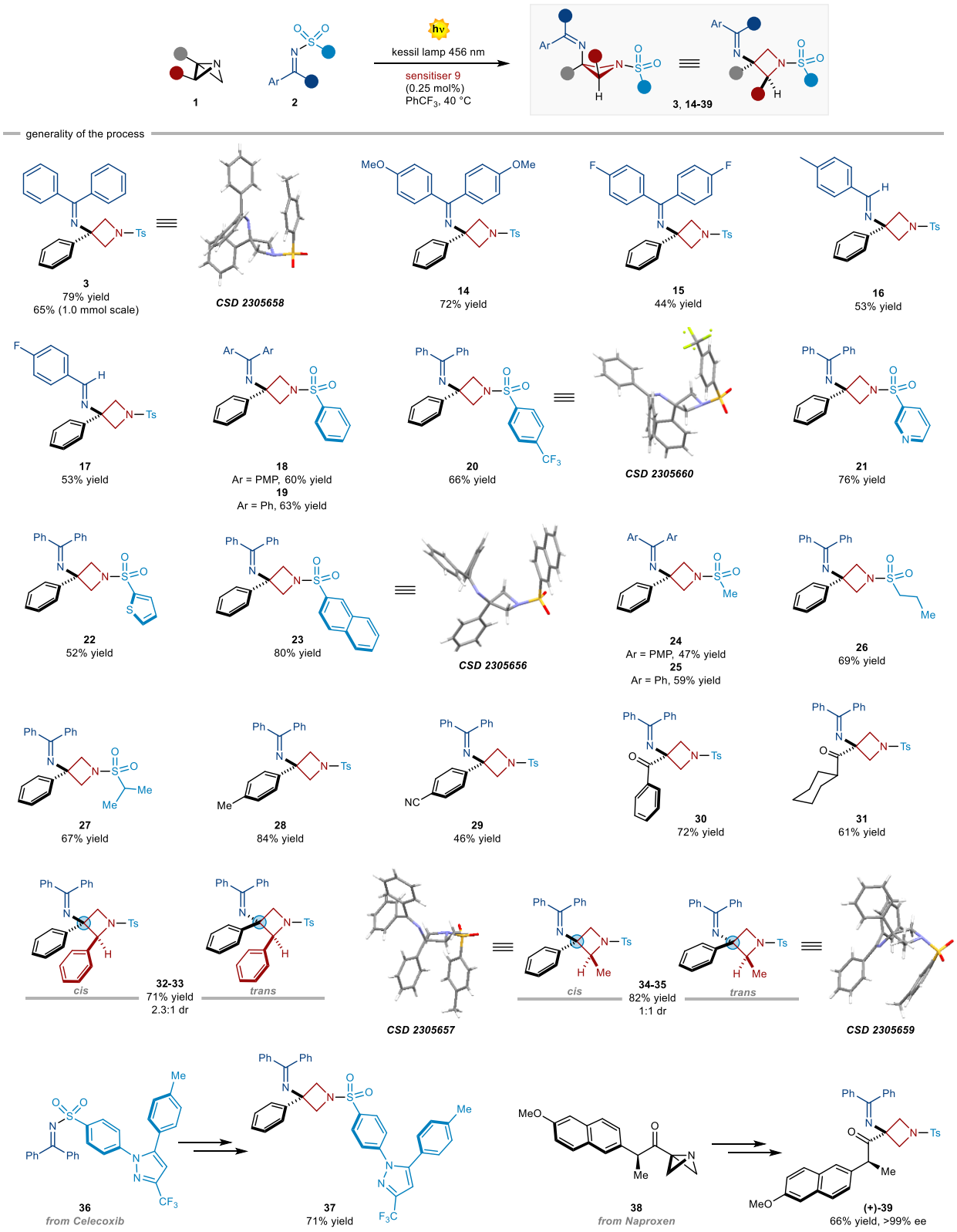

Fig. 4. Generality of the developed method. The reported yields refer to the average of isolated products obtained from three independent reactions. If not otherwise noted the reactions are performed at 0.1 mmol scale. (see Supporting Information for details).

Having shed light on the reaction mechanism, we next evaluated the generality of this RSR photocatalytic process. Diverse types of sulfonylimines turned out to be competent substrates, including ketimine and aldimine precursors with electron-donating (ED) and electron-withdrawing groups (EWGs), affording the azetidine products (**3**, **14**-**19**) in up to 79% yield. Variations at the sulfonyl group were also well tolerated, and the corresponding products **18**-**27** were isolated in yields spanning from 47% to 80%. We next turned our attention to the ABB precursor. Here, diverse aryl and carbonyl groups were evaluated, delivering the corresponding azetidine (**28**-**31**) with yields up to 84%. Also 2-substituted ABBs furnished the products (**32**-**35**) in high yield up to 82%, with a d.r. up to 2.3:1. We obtained crystalline products for both diastereoisomers **34** and **35**. By performing X-ray analysis on the single crystals, we unambiguously inferred their relative configurations. Finally, we applied the developed method to more systems, bearing biologically active scaffolds. Remarkably, the Celecoxib-containing sulfonylimine **36**, as well as the Naproxen-containing ABB **38** reacted smoothly affording the corresponding azetidine products **37** and **39** in 71% and 66% yield, respectively. It is worth mentioning that the mild reaction conditions allowed the preservation of the optical purity of the starting chiral Naproxen derivative **38**.

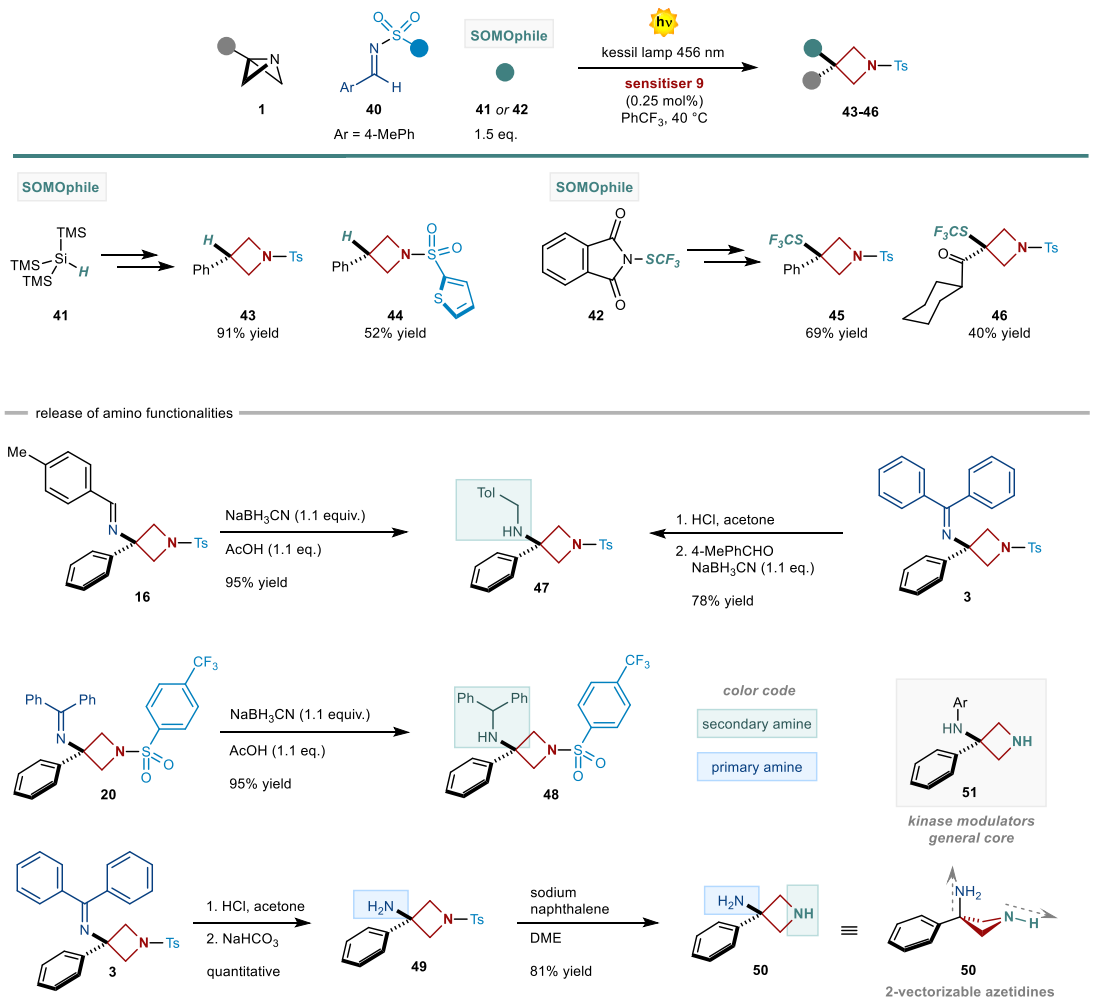

Fig. 5. a) Extension of the method to a three-component reaction with diverse SOMOphiles. b) Release and manipulations of the key amino functionalities of the products.

Having proved the generality of the process for accessing C3-N-type azetidines (Figure 4) through the activity of the key radical intermediate **12** (Figure3), we questioned if it was possible to intercept this transient species with alternative SOMOphiles. Thus, we performed the standard reaction between the ABB **1** and aldimines **40**, in the presence of 1.5 equivalents of the supersilane **41**. Remarkably, the reaction proceeded smoothly accessing compound **43** and **44** in 91% and 52% yield, respectively. Encouraged by this result, and guided by the importance that the SCF_3 moiety represents in pharmaceuticals[46,47], we tested phthalimide-SCF_3 **42**. The reaction led to the corresponding thiotrifluoromethylated azetidines **45** and **46** in 69% and 40% yield, respectively. The latter demonstrate that the designed methodology can easily unlock new types of reactivity while leading access to new families of densely functionalised azetidines without the need of additional optimisation processes.

Finally, we performed some representative synthetic manipulations to unmask the key amino functionalities embodied into the azetidine products. The benzylated intermediate **47** can be accessed by reduction of compound **16** or through reductive amination of **3**. In both cases with very high yields (up to 95%) without the need of any column chromatography. Additionally, benzhydryl amine **48** was obtained through the simple reduction of **20** in 95% yield. Lastly, the amino sulfonylazetidine **49** was obtained through hydrolysis and subsequent neutralisation, without requiring purification steps. Subsequent tosyl group cleavage was accomplished using sodium naphthalene, giving place to the 2-vector 3-aminoazetidine **50**. Remarkably, this 1,2-diamino functionality is present in important classes of kinase modulators **51**.

Conclusions.

To summarise, we have documented that ABB scaffold undergoes radical addition by means of an efficient, mild and chemoselective RSR photocatalytic process leading access to C3-N azetidines with two special vectors (Figure 2 and Figure 4). Mechanistic investigations revealed the key activity of the radical intermediate **12** (Figure 3), generated upon the RSR process. This intermediate was further exploited in the presence of diverse SOMOphilic species (**41** and **42** in Figure 5) furnishing the corresponding C3-H and C3-S azetidine derivatives.

Another key aspect in this new synthetic platform is the selection and design of the sensitiser, characterised by the shortest ΔS_1T_1 reported for an organic molecule. We speculated that the negligible difference between the S_1 and T_1 energy favours an ideal balance between the inactive and active PC's excited state species, resulting in the finely controlled sulfonylimine activation. Furthermore, the reaction requires as little as 0.25 mol% catalyst loading, resulting in an extremely efficient and sustainable energy transfer process. Finally, the performed synthetic manipulations highlighted the power of this process in accessing key building blocks for biologically relevant azetidines. Based on the reported results, we foreseen the utilisation of the ABB scaffolds in other types of RSR processes expanding the synthetic repertoire for azetidines construction.

Acknowledgements

This work was supported by MUR (Ministero dell'Università) PRIN 2020927WY3_002, and (European Research Council) ERC-Starting Grant 2021 SYNPHOCAT 101040025 (L.D.). Chiesi Farmaceutici SpA and Dr Davide Balestri are acknowledged for the support with the D8 Venture X-ray equipment.

References

1) Vitaku, E.; Smith, D. T. & Njardarson, J. T. Analysis of the Structural Diversity, Substitution Patterns, and Frequency of Nitrogen Heterocycles among U.S. FDA Approved Pharmaceuticals. *J. Med. Chem*. **57**, 10257−10274 (2014).
2) Ricci, A., Ed., Amino Group Chemistry: From Synthesis to the Life Sciences (Wiley-VCH, Weinheim, Germany, 2008).
3) Bhutani, P.; Joshi, G.; Raja, N.; Bachhav, N.; Rajanna, P. K.; Bhutani, H.; Paul, A. T. & Kumar, R. U.S. FDA Approved Drugs from 2015–June 2020: A Perspective *J. Med. Chem*. **64**, 2339-2381 (2021).
4) Lovering, F., Bikker, J., Humblet, C. Escape from Flatland: Increasing Saturation as an Approach to Improving Clinical Success. *J. Med. Chem*., **52**, 6752-6756 (2009).
5) Lovering, F. Escape from Flatland 2: complexity and promiscuity. *MedChemComm*, **4**, 515-519 (2013).
6) St. Jean, D. J. & Fotsch, C. Mitigating heterocycle metabolism in drug discovery. *J. Med. Chem*. **55**, 6002–6020 (2012).
7) Shu, Y.-Z., Johnson, B. M. & Yang, T. J. Role of biotransformation studies in minimizing metabolism-related liabilities in drug discovery. *AAPS J*. **10**, 178–192 (2008).
8) Andresini, M., Degennaro, L., Luisi, R. The renaissance of strained 1-azabicyclo[1.1.0]butanes as useful reagents for the synthesis of functionalized azetidines *Org. Biomol. Chem*. **18**, 5798-5810 (2020).
9) Antermite, D., Degennaro, L. & Luisi, R. Recent advances in the chemistry of metallated azetidines. The renaissance of strained 1-azabicyclo[1.1.0]butanes as useful reagents for the synthesis of functionalized azetidines. *Org. Biomol. Chem*. **15**, 34–50 (2017).
10) Maetani, M.; Zoller, J.; Melillo, B.; Verho, O.; Kato, N.; Pu, J.; Comer, E.; Schreiber, S. L. Synthesis of a Bicyclic Azetidine with In Vivo Antimalarial Activity Enabled by Stereospecific, Directed C(sp(3))-H Arylation. *J. Am. Chem. Soc*. **139**, 11300−11306 (2017).
11) Integrity, https://integrity.clarivate.com/integrity/xmlxsl/pk_ home.util_home, (accessed January 2023).
12) Rice, K. D.; Aay, N.; Anand, N. K.; Blazey, C. M.; Bowles, O. J.; Bussenius, J.; Costanzo, S.; Curtis, J. K.; Defina, S. C.; Dubenko, L.; Engst, S.; Joshi, A. A.; Kennedy, A. R.; Kim, A. I.; Koltun, E. S.; Lougheed, J. C.; Manalo, J.-C. L.; Martini, J.-F.; Nuss, J. M.; Peto, C. J.; Tsang, T. H.; Yu, P.; Johnston, S. Novel Carboxamide-Based Allosteric MEK Inhibitors: Discovery and Optimization Efforts Toward XL518 (GDC-0973). *ACS Med*. *Chem. Lett*. **3**, 416− 421 (2012).
13) Oizumi, K.; Nishino, H.; Koike, H.; Sada, T.; Miyamoto, M.; Kimura, T. Antihypertensive Effects of CS-905, a Novel Dihydropyridine Ca+2 Channel Blocker. *Jpn. J. Pharmacol*. **51**, 57−64 (1989).
14) Bauer, M. R.; Di Fruscia, P.; Lucas, S. C. C.; Michaelides, I. N.; Nelson, J. E.; Storer, R. I.; Whitehurst, B. C. Put a ring on it: application of small aliphatic rings in medicinal chemistry. *RSC Med. Chem*. **12**, 448-471 (2021).

15) Quinodoz, P.; Drouillat, B.; Wright, K.; Marrot, J.; Couty, F. *N*-Arylazetidines: Preparation through Anionic Ring Closure. *J. Org. Chem*. **81**, 2899−2910 (2016).
16) Kovács, E.; Faigl, F.; Mucsi, Z. Regio- and Diastereoselective Synthesis of 2-Arylazetidines: Quantum Chemical Explanation of Baldwin's Rules for the Ring-Formation Reactions of Oxiranes. *J. Org. Chem*. **85**, 11226−11239 (2020).
17) Betz, K. N.; Chiappini, N. D.; Du Bois, J. Intermolecular sp^3-C-H Amination for the Synthesis of Saturated Azacycles. *Org. Lett*. **22**, 1687−1691 (2020).
18) Alcaide, B.; Almendros, P.; Aragoncillo, C. β-Lactams: versatile building blocks for the stereoselective synthesis of non-β-lactam products. *Chem. Rev*. **107**, 4437−4492 (2007).
19) Pitts, C. R.; Lectka, T. Chemical synthesis of β-lactams: asymmetric catalysis and other recent advances. *Chem. Rev*. **114**, 7930−7953 (2014).
20) Franceschi, P., Cuadros, S., Goti, G., Dell'Amico, L. Mechanisms and Synthetic Strategies in Visible-Light-Driven [2+2]-Heterocycloadditions. *Angew. Chem. Int. Ed.* **62**, e202217210 (2023).
21) Richardson, A. D.; Becker, M. R.; Schindler, C. S. Synthesis of azetidines by aza Paterno-Buchi reactions. *Chem. Sci*. **11**, 7553− 7561 (2020).
22) Rykaczewski, K. A.; Becker, M. R.; Anantpur, M. J.; Sausa, R. C.; Johnson, E. C.; Orlicki, J. A.; Bukowski, E. J.; Sabatini, J. J.; Schindler, C. S. Photochemical Strategies Enable the Synthesis of Tunable Azetidine-Based Energetic Materials. *J. Am. Chem. Soc.* **144**, 19089−19096 (2022).
23) Becker, M. R.; Wearing, E. R.; Schindler, C. S. Synthesis of azetidines via visible-light-mediated intermolecular [2+2] photocycloadditions. *Nat. Chem*. **12**, 898−905 (2020).
24) Blackmun, D. E.; Chamness, S. A.; Schindler, C. S. Intramolecular, Visible-Light-Mediated Aza Paterno-Buchi Reactions of Unactivated Alkenes. *Org. Lett*. **24**, 3053−3057 (2022).
25) Lopchuk, J. M.; Fjelbye, K.; Kawamata, Y.; Malins, L. R.; Pan, C. M.; Gianatassio, R.; Wang, J.; Prieto, L.; Bradow, J.; Brandt, T. A.; Collins, M. R.; Elleraas, J.; Ewanicki, J.; Farrell, W.; Fadeyi, O. O.; Gallego, G. M.; Mousseau, J. J.; Oliver, R.; Sach, N. W.; Smith, J. K.; Spangler, J. E.; Zhu, H.; Zhu, J.; Baran, P. S. Strain-Release Heteroatom Functionalization: Development, Scope, and Stereospecificity. *J. Am. Chem. Soc*. **139**, 3209−3226 (2017).
26) Gianatassio, R.; Kadish, D. Direct Alkylation of 1- Azabicyclo[1.1.0]butanes. *Org. Lett*. **21**, 2060−2063 (2019).
27) Fawcett, A.; Murtaza, A.; Gregson, C. H. U.; Aggarwal, V. K. Strain-Release-Driven Homologation of Boronic Esters: Application to the Modular Synthesis of Azetidines. *J. Am. Chem. Soc*. **141**, 4573−4578 (2019).
28) Funke, W. Synthesis and properties of 1-azabicyclo [1.1. 0] butanes. *Angew. Chem., Int. Ed.* Engl., **8**, 70−71 (1969).
29) Gianatassio, R.; Lopchuk, J. M.; Wang, J.; Pan, C.-M.; Malins, L. R.; Prieto, L.; Brandt, T. A.; Collins, M. R.; Gallego, G. M.; Sach, N. W.; Spangler, J. E.; Zhu, H.; Zhu, J.; Baran, P. S. Strain-release amination. *Science* **351**, 241−246 (2016).
30) Musci, P.; Colella, M.; Andresini, M.; Aramini, A.; Degennaro, L.; Luisi, R. Flow technology enabled preparation of C3-heterosubstituted 1-azabicyclo[1.1.0]butanes and azetidines: accessing unexplored chemical space in strained heterocyclic chemistry. *Chem. Commun*. **58**, 6356−6359 (2022).
31) Hsu, C.-M.; Lin, H.-B.; Hou, X.-Z.; Tapales, R. V. P. P.; Shih, C.-K.; Miñoza, S.; Tsai, Y.-S.; Tsai, Z.-N.; Chan, C.-L.; Liao, H.-H., Azetidines with All-Carbon Quaternary Centers: Merging Relay Catalysis with Strain Release Functionalization. *J. Am. Chem. Soc*. **145**, 19049−19059 (2023).
32) Narayanam, J. M. R.; Stephenson, C. R. J. Visible light photoredox catalysis: applications in organic synthesis. *Chem. Soc. Rev*. **40**, 102-113 (2011).

33) Prier, C. K.; Rankic, D. A.; MacMillan, D. W. C. Visible Light Photoredox Catalysis with Transition Metal Complexes: Applications in Organic Synthesis. *Chem. Rev*. **113**, 5322-5363 (2013).
34) Meggers, E. Asymmetric catalysis activated by visible light. *Chem. Commun*. **51**, 3290-3301 (2015); d) Shaw, M. H., Twilton, J.; MacMillan, D. W. C. Photoredox Catalysis in Organic Chemistry. *J. Org. Chem.* **81**, 6898-6926 (2016).
35) Skubi, K. L.; Blum, T. R.; Yoon, T. P. Dual Catalysis Strategies in Photochemical Synthesis. *Chem. Rev*. **116**, 10035-10074 (2016).
36) Romero, N. A.; Nicewicz, D. A. Organic Photoredox Catalysis. *Chem. Rev*., **116**, 10075-10166 (2016).
37) Dutta, S., Erchinger, J. E., Strieth-Kalthoff, F., Kleinmans, R., Glorius, F. Energy transfer photocatalysis: exciting modes of reactivity. *Chem. Soc. Rev*., doi: 10.1039/D3CS00190C (2023).
38) Belloti, P., Glorius, F., Strain-Release Photocatalysis, *J. Am. Chem. Soc.* **145**, 20716−20732 (2023).
39) Marson, C. M. New and unusual scaffolds in medicinal chemistry, *Chem. Soc. Rev*. **40**, 5514–5533 (2011).
40) Lowe, J. T.; Lee, M. D. t.; Akella, L. B. *et. al*. Synthesis and profiling of a diverse collection of azetidine-based scaffolds for the development of CNS-focused lead-like libraries. J*. Org. Chem.* **77**, 7187−7211 (2012).
41) Mateos, J., Rigodanza, F., Costa, P. *et al.* Unveiling the impact of the light source and steric factors on [2 + 2] heterocycloaddition reactions. *Nat. Synth* **2**, 26–36 (2023).
42) Mateos, J., Vega-Peñaloza, A., Franceschi, P., Rigodanza, F., Andreetta, P., Pelosi, G., Companyó, X., Bonchio, M., Dell'Amico, L. A visible-light Paternò–Büchi Dearomatisation Process Towards the Construction of Oxeto-Indolinic Polycycles. *Chem. Sci.* **11**, 6532-6538 (2020).
43) Strieth-Kalthoff, F., James, M. J., Teders, M., Pitzer, L., Glorius, F. Energy transfer catalysis mediated by visible light: principles, applications, directions. *Chem. Soc. Rev.* **47**, 7190-7202 (2018).
44) Thoi, H. H.; Ito, O.; Iino, M.; Matsuda, M. Studies of sulfonyl radicals. 4. Flash photolysis of aromatic sulfones. *J. Phys. Chem*. **82**, 314-319 (1978).
45) Ortica, F.; Coenjarts, C.; Scaiano, J. C., Liu, H.; Pohlers, G.; Cameron, J. F. Mechanism of Reaction and Photoacid Generation of N-Oxysuccinimidoarylsulfonate PAGs: A Laser Flash Photolytic Study *Chem. Mater*. **13**, 2297-2304 (2001).
46) Meanwell, N. A., Fluorine and fluorinated motifs in the design and application of bioisosteres for drug design. *J. Med. Chem*. **61**, 5822-5880 (2018).
47) Zhou, Y.; Wang, J.; Gu, Z.; Wang, S.; Zhu, W.; Acena, J. L.; Soloshonok, V. A.; Izawa, K.; Liu, H. Next generation of fluorine-containing pharmaceuticals, compounds currently in phase II-III clinical trials of major pharmaceutical companies: new structural trends and therapeutic areas. *Chem. Rev*. **116**, 422-518 (2016).